WHY SAR WAVE MODE DATA OF ERS AND ENVISAT ARE INADEQUATE FOR GIVING THE PROBABILITY OF OCCURRENCE OF FREAK WAVES

Peter Janssen[1] and Werner Alpers[2]

[1] *ECMWF, Shinfield Park, Reading RG2 9AX, United Kingdom*
[2] *Institut für Meereskunde, Universität Hamburg, Bundesstrasse 53, D-20146 Hamburg, Germany*

ABSTRACT

It would be highly desirable to have a global monitoring tool for the detection of freak or rogue ocean surface waves. Based on the SAR imaging theory of ocean surface waves developed already in the 1980's, it is argued that unfortunately, despite recent claims to the contrary, this is not possible using SAR wave mode data of the ERS and Envisat satellites. The main reason for this is that, due to the motion of the sea surface, the SAR imaging mechanism is, in general, strongly nonlinear. Thus the SAR image of the ocean wave field is a highly distorted image of the ocean wave field which bears little resemblance with the actual ocean wave field. Exceptions are perhaps cases where narrow-band swell trains propagate in range direction in the absence of a wind sea. However, these cases are rare and cannot serve as representative samples for the global distribution of possible sea states. The locations of the maxima in the SAR image intensity or the "groupiness" in the image intensity distribution do not, in general, represent the locations of maxima in the wave amplitude or "groupiness" in the actual ocean wave field. Thus it is impossible to obtain with this technique reliable information on the occurrence probability of extreme ocean waves on a global scale.

1 INTRODUCTION

Nowadays there is an increased understanding of the reasons why freak waves on the ocean surface are generated. On the open ocean freak waves are generated by nonlinear focussing. Freak waves have been simulated numerically (in 1D and even in 2 D) and have been generated in the laboratory. Prompted by the theoretical evidence, experimentalists had another look at their observed time series from wave buoys. They found that extreme sea states occurred more frequently then previously thought. A key issue here is that probably in the past a too strict quality control to the time series for the surface elevation was applied which had the effect that many cases of extreme sea state were removed from the statistics.

Since ships, oil rigs, etc. have not been designed to withstand these exceptional high surface waves, it is of the utmost importance to be able to predict the occurrence of freak waves. Modern wave forecasting systems determine the evolution of the ocean wave spectrum, but do not provide information on the phases of the waves. Hence, it is not possible to predict individual wave events. However, recently it has been realized [1] that the nonlinear four-wave interactions imply a relationship between spectral shape and the deviation of the surface elevation probability distribution function (pdf) from the normal Gaussian distribution. Here large deviations with positive kurtosis correspond to the likely occurrence of freak waves. In one dimension, this theory has been succesfully validated against laboratory observations from the big wave tank in Trondheim, Norway. Therefore, we can predict the probability that extreme or freak waves do occur (probablistic wave forecasting). As a consequence, at the European Centre for Medium Range Weather Forcast (ECMWF) a freak wave warning system has been implemented in October 2003.

Clearly, it is highly desirable to validate the present theory of freak wave formation on a global scale. In this paper we argue that this unfortunately is not possible by using synthetic aperture radar (SAR) images acquired in the wave mode by the European Remote Sensing satellites ERS-1 and ERS-2 and the Envisat satellite. The main reason for this is that the SAR imaging mechanism of ocean surface waves is, in general, strongly nonlinear due to velocity bunching and azimuthal image smear [2], [3], which leads to a highly distorted images that have very little resemblance with the original ocean wave elevation field.

This paper is organized as follows: In Section 2 we give a brief review of the present theory of freak wave generation. On the open ocean, extreme waves are generated by nonlinear focussing, a process that also causes the well-known Benjamin-Feir Instability. Nonlinear focussing is caused by four wave interactions which are the most efficient when the waves are nonlinear and coherent. A wave system is coherent when the wave spectrum is narrow. In Section 3 we review briefly the SAR imaging mechanism of ocean surface waves and point out its limitations. In general, the motion of the ocean surface prevents that there is a simple, linear relationship between SAR image intensity and the ocean surface elevation (or ocean wave) field. Ocean waves propagating in flight (azimuthal) direction and having a wavelength below a certain cutoff wavelength (which depends, among others, on significant waveheight) are not imaged by SAR. As a consequence, SAR observes a too narrow ocean wave spectrum. Thus the sea state measured by SAR is more coherent than the actual sea state, which leads to an

artificial increase of the number of freak waves. In order to illustrate that the ocean wave fields and the corresponding SAR image intensity fields look, in general, quite different, we present in Section 4 two examples of SAR imaging of ocean waves. In these examples we have approximated the relationship between ocean wave and SAR image intensity spectra by an azimuthal filter, which acts on the ocean wave spectrum, and have ignored tilt, hydrodynamic and range bunching modulations. If we would have applied the full SAR imaging mechanism, then ocean wave fields and the SAR image intensity fields would have looked even more dissimilar. These examples clearly show that it is not permissible to view the SAR image as being a "true" image of the sea surface elevation field. Furthermore, we show in Section 5 that the peakedness parameters of ocean wave spectra derived from Envisat level 2 ASAR wave mode products are much smaller than the ones calculated from the WAM wave prediction model, although the WAM peakedness parameters correlate well with buoy-derived ones. From this observation we conclude that the widths of the ocean wave spectra provided by the Envisat ASAR level 2 ASAR products are too narrow and that they are problematic when using them for identifying ocean regions with narrow wave spectra, where the probability of encountering freak waves is enhanced. Finally, in Section 6 we summarize the results of the paper and point out that the claim of Lehner (DLR) and Rosenthal (GKSS) that they have detected on ERS SAR wave mode data several freak or rogue waves with waveheights above 25 m [4], [5] has no scientific basis.

2 FREAK WAVE GENERATION

The systematic study of the generation mechanisms of freak waves only started some 15 years ago, but already there is a reasonable understanding under what conditions freak waves occur. In the 1980's it was well-known that there are a number of linear mechanisms that may give rise to focussing of wave energy. Examples are refraction of wave energy by bottom topography and by currents, and diffraction of wave energy behind islands. But also nonlinear interactions may result in focussing.

First numerical simulations (using phase resolving numerical models) and experiments were done by Japanese groups in the early 1990's [6] – [8]. From these works the picture emerged that nonlinear focussing enhances the appearance of freak waves and are the primary cause of freak wave generation in a general wave field. This finding was confirmed by European groups [9], [10] at the end of the 1990's and the beginning of the 21st century. These works are primarily concerned with the formation of individual extreme events and the main aim was exploring the conditions under which these extreme events occur. The main interest here is in forecasting of extreme conditions. Now, operational wave forecasting is based on an ensemble averaged, or phase averaged, description of the sea state. At best, we can give statements on the probability of occurrence of freak waves. Hence, a connection between the generation of freak waves and the probability distribution function of the surface elevation needs to be established.

Linear waves on the open ocean are independent and therefore the Random Phase Approximation applies. This means that, in a good approximation, ocean waves follow Gaussian statistics. In linear theory focussing is caused by constructive interference, which gives at best a doubling of the amplitude. However, the situation for nonlinear waves is entirely different, because now there is the possibility of wave-wave interaction. Thus, a wave may borrow energy from its neighbours. Because of this extra focussing, wave height may become 5 – 6 times as large as the average wave height. As a consequence, for nonlinear waves, the surface elevation distribution is rather different, in particular for the extremes.

The kurtosis C_4, which measures deviations from the Normal Distribution, can be expressed in terms of the wave spectrum [11], and therefore, for a given sea state, the probability of occurrence of extreme wave events can be obtained. Hence,

$$C_4 = \langle \eta^4 \rangle / 3 \langle \eta^2 \rangle^2 - 1 = \text{function(seastate)}.$$

Note that we have defined kurtosis here in such a way that it vanishes for a Gaussian sea state. Further analysis shows that for narrow-band waves C_4 depends on two parameters, namely the Benjamin-Feir Index (BFI) and the angular width $\Delta \theta$ of the spectrum. Here, the BFI is defined as the ratio of a typical steepness and the width of the frequency spectrum,

$$BFI = \epsilon \sqrt{2} / \sigma'_\omega,$$

where

$$\sigma'_\omega = \sigma_\omega / \omega_0$$

is the relative width of the frequency spectrum and

$$\epsilon = (k_0^2 < \eta^2 >)^{\frac{1}{2}}$$

is an integral measure of wave steepness (with $< \eta^2 >$ the average surface elevation variance and k_0 the peak wave number). Nonlinear focussing is promoted when the BFI is large and $\Delta \theta$ is small. In other words, extreme waves

are likely to occur for a steep, coherent sea states. The theoretical picture has been confirmed by laboratory observations obtained in a Japanese wave tank [12] and in a large wave tank in Trondheim [13]. In Fig. 1 the theoretical pdf of wave height is compared with an observed record from the Trondheim wave tank for a case of strong nonlinear focussing with BFI = 1.2. Note that a well-accepted definition of an extreme sea state is one where wave height exceeds twice the average significant wave height of the surrounding wave field. It is then evident from Fig. 1 that in this strongly nonlinear case it is very likely to expect extreme waves as at $H/H_s=2$ the pdf is 10 times larger than the one from linear theory (Rayleigh distribution). And indeed, the time series showed evidence of the generation of freak waves.
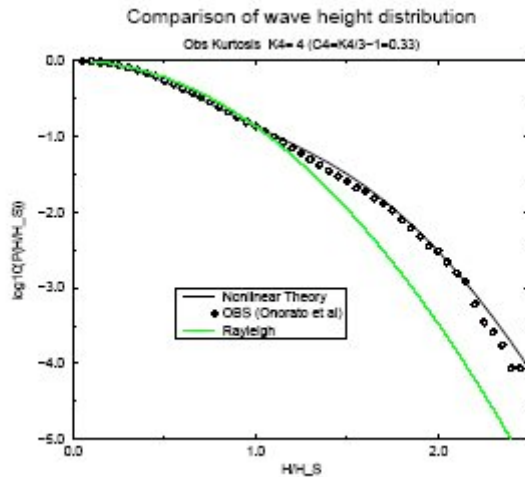
Fig.1: Comparison of theoretical and observed wave height distribution [13]. For reference, the linear Rayleigh result is shown as well.

3 SAR IMAGING OF OCEAN WAVES

3.1 The freak wave issue

It is highly desirable to have a global monitoring tool to detect extreme events, such as freak waves are. Recently Lehner [4]and Rosenthal [5] claimed that they have detected on a global set of ERS-2 SAR wave mode data (consisting of 34000 imagettes acquired over a period of 27 days in 1996 and 1996) several freak or rogue waves with waveheights above 25 m [4]. However, no proof of this claim has been given. Rather Nieto Borge et al. [14] and Niedermayer et al. [15] produced global maps of grouping parameters obtained from SAR images. But, on a global scale it is not permissible to assume that the ocean surface elevation field is linearly related to the SAR image intensity. In [15] it is stated that for the range travelling case the group structure of the wave field, i. e., the size and the relative position of the groups, is well represented in the SAR image. Under certain conditions, this may be true for the case of long waves travelling close to range direction, but it is not true for waves travelling in the other directions. On a global ocean, ocean waves propagate in all directions. Their argument cannot be used as a justification for applying the results of their image processing techniques to a global data set with the aim of obtaining useful information on the distribution of freak waves on the World's ocean. In general, due to the nonlinearity of the SAR imaging mechanism, the group structure of the ocean wave field is quite different from the group structure of the SAR image intensity field. Groupiness detected on SAR images do not, in general, match groupiness and maximum wave height in the ocean wave field. In any case, their image processing techniques cannot be applied to a global data set where all kinds of ocean waves are encountered propagating in all directions. Thus this technique yields no useful information on the distribution of freak waves on the World's ocean.
In a recent paper Schulz-Stellenfleth and Lehner [16] have proposed a method for extracting sea surface elevation fields from complex SAR data. However, this method uses a quasi-linear transform which applies only when the waves travel close to range direction. They smooth the SAR spectrum in the azimuth direction which leads to severe artefacts in the retrieved ocean wave field. The authors give no proof that their method is applicable for extracting information on freak waves from a global wave mode data set that does not contain only near range travelling ocean waves. But even for range travelling waves this method cannot be applied for detecting freak waves, because they make the assumption that the modulation of the normalized radar cross section (NRCS) is linearly related to the sea surface elevation, which cannot be valid when SAR images extreme waves. In this case the waves break and the scatter elements move with a faster speed (phase speed) than the orbital velocity.

3.2 Basics of the SAR imaging mechanism of ocean waves

In order to explain this in more detail we review briefly the main features of the SAR imaging mechanism of ocean surface waves. For low to moderate sea states, the modulation of the SAR image intensity is caused by (1) modulation of the normalized cross section (NRCS) consisting of tilt, and hydrodynamic modulations, (2) by range bunching modulation, and (3) by motion-induced modulations [17],[18]. The most important contribution to the motion-induced modulation is "velocity bunching" [2], [3], [19]. It is related to the use of phase information by the SAR to locate the azimuthal position of scattering elements (facets). The SAR positions the facet always at the azimuthal location of zero Doppler shift. The orbital motion of a facet (caused by the long ocean waves) induces an additional Doppler shift which is misinterpreted by SAR as an azimuthal offset of the position of the facet. This is accompanied by variations in the apparent facet density in the SAR image, which enables waves to be seen even when no NRSC modulation is present.

The azimuthal displacement is proportional to the product of the radial component of the orbital velocity of the waves and the range (R) to velocity (V) ratio, $\beta=R/V$, of the SAR platform. In particular, for polar orbiting platforms with $\beta = O(100)$ s the velocity bunching effect is a serious issue. When the displacement is small compared to the length of the ocean wave of interest, the velocity bunching effect is linear. However, if the facet displacement becomes comparable or larger than the length of the longer ocean waves, the wave patterns in the SAR image become severely distorted and can even be completely smeared out. This ultimately limits the azimuthal resolution of the SAR at a finite cutoff wavenumber. This is illustrated in Fig.2 for increasing nonlinearity (e.g. for increasing wave amplitude).
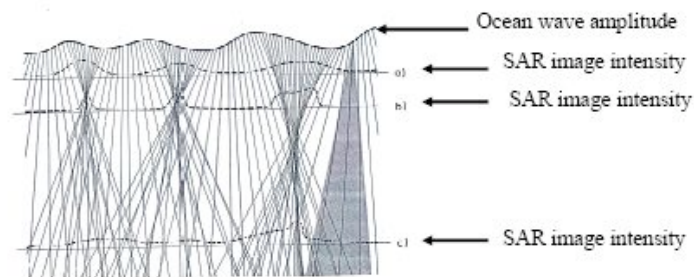
Fig.2: Azimuthal displacement of a facet in the SAR image plane due to the long wave orbital velocity; a) linear imaging; b) nonlinear imaging, c) strongly nonlinear imaging.

The velocity bunching mechanism is a purely geometrical, fully determined process. If the other contributions to the SAR image intensity modulations are known, then the mapping of the sea surface into the SAR image plane and the nonlinear transformation of the wave spectrum into the SAR image spectrum can be computed for a given realization of the ocean wave field. This is the basis of the Monte Carlo approach of Bruening et al. [20], [21], where for a given ocean wave spectrum a number of random realizations of an instantaneous ocean wave field are generated. For each member of the ensemble, the sea surface is mapped into the SAR image plane. Fourier transformation of the image and averaging of the squared amplitudes then gives an estimate of the SAR image variance spectrum. In Fig. 3 an example of such a Monte Carlo simulation of a SAR image spectrum is depicted which shows that SAR (here flown on the Spaceshuttle which had at this flight a low value of β of about 30 s) distorts the actual surface wave spectrum to a considerable extent. Note that the spectral peak in the SAR spectrum is rotated towards range direction (vertical axis). This shift of the wave direction was confirmed by comparing the SAR image spectum with an ocean wave spectrum measured by a wave buoy.
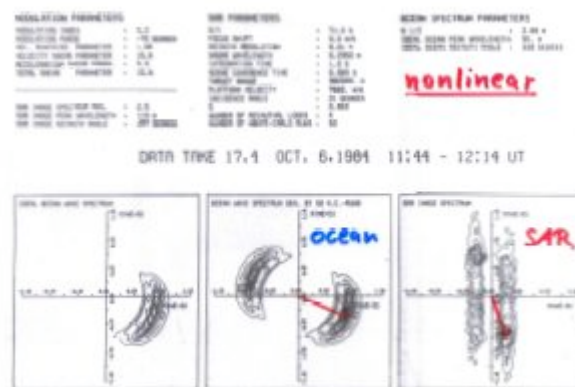
Fig. 3: Ocean wave imaging from Spaceshuttle. The SAR image spectrum is highly distorted. In particular, the spectral peak is rotated in the SAR spectrum towards the range direction (vertical axis).

3.3 Azimuthal cutoff

While the orbital motion of the long ocean waves with an azimuth component allows the waves to be imaged through the velocity bunching mechanism, the random motions of the ocean surface caused by the shorter scale waves introduce random shifts in azimuth that in turn degrade the azimuth resolution. In short, the SAR acts like a low-pass filter because waves with an azimuth wavelength shorter than λ_{min} are not detected by SAR. Beal et al. [22] used a Gaussian shaped low-pass filter and found a semi-empirical relationship for the minimum detectable wavelength, which depends on significant wave height H_s and on $\beta = R/V$. Here, we will use a slightly more general approach based on the work of Hasselmann and Hasselmann [18] who find that for a Gaussian sea the effects of velocity bunching on the SAR image spectrum are indeed given by means of a Gaussian-shaped low pass azimuthal filter function G. Adopting from now on the convention that the range is in the x-direction while the azimuth is in the y-direction, we have

$$G(k_y) = \exp\left(-k_y^2/k_c^2\right)$$

where the cutoff wavenumber is defined as

$$\frac{1}{k_c^2} = \beta^2 \int d\vec{k} \; |T^v(\vec{k})|^2 F(\vec{k}).$$

Here, $T^v(\mathbf{k})$ is the range orbital velocity transfer function [3] and $F(\mathbf{k})$ is the wavenumber spectrum of the ocean surface waves. For the relatively small incidence angles (of the order of 20 degrees) at which the SARs on board the ERS 1/2 and ENVISAT satellites are operating, the expression for the azimuthal cutoff wavenumber may be simplified [23] since directional aspects of the wave field can be shown to have a small impact. As a result, the cutoff wavenumber is in good approximation proportional to the vertical component of the orbital velocity, and given by

$$\frac{1}{k_c^2} = \beta^2 \int d\vec{k} \; \omega^2 F(\vec{k}).$$

Note that, following [24], the SAR azimuth cutoff wavelength λ_{min} is defined as $\lambda_{min} = \pi/k_c$. In a similar vain as in [22], it is straightforward to obtain a realistic estimate of the azimuth cutoff wavelength by using the well-known Phillips' spectrum

$$F(k) = \frac{\alpha_p}{2} k^{-3}$$

for $k > k_p = \omega_p^2/g$. Here ω_p denotes the angular peak frequency and α_p denotes the Phillips' parameter.
For the typical case of an old wind sea, the waves at the peak of the wave spectrum have a phase speed that matches the wind speed at 10 m height, U_{10}. As a consequence, λ_{min} becomes

$$\lambda_{min} = \beta \pi U_{10} \sqrt{\alpha_p/2} \simeq 25 U_{10}$$

The last approximation follows from typical values: $\beta = 115$ s, and $\alpha_p = 0.01$. Even for fairly low wind speeds of 5 m/s one finds already quite long azimuthal cutoff wavelengths of the order of 125 m, while for the climatogical mean wind speed of 7.5 m/s one finds $\lambda_{min} = 188$ m. This suggests that the loss of azimuth resolution by the velocity bunching mechanism is a serious problem for imaging ocean waves by means of SAR.

3.4 Nonlinearity

The SAR imaging of ocean waves has been based on linear arguments. Consequently, the pdf of the sea surface elevation was taken as a Gaussian, which is consistent with the assumption that waves are linear. However, for extreme waves the SAR imaging mechanism is expected to be highly nonlinear because of the breakdown of the linear relationship between wave amplitude and cross section modulation. This applies also to range travelling ocean waves.
In addition, the assumption of a normally distributed surface elevation may not be valid in case of freak waves [11]
For example, in the Hasselmann and Hasselmann approach [18] the effect of velocity bunching in wavenumber space is obtained by determining the ensemble average of

$$N_k = \exp\left(-i\vec{k}.\vec{\zeta}\right)$$

where $\zeta = \xi(\mathbf{r_1}) - \xi(\mathbf{r_2})$ is the difference in azimuthal displacement ξ at two locations $\mathbf{r_1}$ and $\mathbf{r_2}$, respectively. For a Gaussian sea one readily finds

$$\langle N_k \rangle = \langle \exp\left(-i\vec{k}.\vec{\zeta}\right)\rangle = \exp\left(-\frac{1}{2}k^2 \langle \vec{\zeta}^2 \rangle\right)$$

This is a straightforward calculation because the ensemble average of N_k is nothing but the so-called characteristic function of the pdf of ζ, which in fact is the Fourier transform of the pdf.
Note that

$$\langle \vec{\zeta}^2 \rangle / 2 = 1/k_c^2$$

Hence, in wavenumber space, the low-pass filter which represents the velocity bunching effect is just the Fourier transform of the pdf of the stochastic process ζ.
Therefore, for a Gaussian sea the azimuthal low-pass filter is a Gaussian, and this is in most cases expected to be an adequate model. For extreme events, however, the pdf is non-normal and deviations in the shape of the azimuthal low-pass filter are expected. In order to illustrate this point, deviations from normality are modelled by means of an Edgeworth distribution [11] but ignoring effects of skewness. The pdf for the azimuthal displacement ξ then becomes

$$p(\xi) = \left[1 + \frac{\sigma^4 C_4}{8} \frac{\mathrm{d}^4}{\mathrm{d}\xi^4}\right] f_0(\xi),$$

where

$$f_0 = \exp\left(-\xi^2/2\sigma^2\right)/\sigma\sqrt{2\pi}$$

is the normal distribution with variance σ^2, while C_4 is the kurtosis parameter for the displacement ξ.
The ensemble average of N_k now becomes

$$\langle N_k \rangle = \exp\left(-k^2/k_c^2\right)\left[1 + \frac{C_4}{4}\left(\frac{k}{k_c}\right)^4\right]$$

with $k_c = 1/\sigma$. The effect of finite positive kurtosis is to broaden the low-pass filter in the wavenumber space. This suggests that by studying the shape of the azimuthal low-pass filter one can, in principle, infer statistical parameters, such as skewness and kurtosis, and thus obtain information on the occurrence of extreme sea states. However, changes in the shape of the low-pass filter are relatively small; the extreme case of $C_4 = 0.5$ would only give a decrease in the azimuthal cutoff wavelength of 10 %. In addition, the above result is only an indication of the expected impact of deviations from Normality, as effects of skewness on the nonlinear SAR mapping transform should be taken into account as well. Work in this direction is under way.

4 EXAMPLES OF SAR IMAGES

One would expect that the distortions produced by the SAR imaging are minimal when waves are travelling in the range direction, because these do not suffer from the velocity bunching effect. Therefore, Nieto Borge et al. [14] claim that their wave group analysis is valid for nearly range travelling waves, but even this can be questioned because (1) the low-pass filter produces in the azimuth direction a too narrow spectrum and (2) the nonlinearity and velocity bunching rotates the waves in the SAR image towards the range direction. These effects cause that the SAR observes a much narrower wave spectrum than is present in reality. Hence, SAR measures a more coherent wave system and thus it is more likely to find extreme events in SAR images (as the effects of destructive interference are reduced by the low-pass filtering).
In order to illustrate some of the problems with SAR imaging of ocean waves we have simulated two maps of sea surface elevation and calculated the corresponding SAR image intensity maps by using a simplified SAR imaging model of ocean waves. Since our aim is to solely illustrate the effect of velocity bunching on the SAR imaging of ocean waves, we neglect for this purpose the effects of tilt, hydrodynamic, and range bunching modulations and relate the SAR image intensity spectrum P($\mathbf{k}$) to ocean wave spectrum F($\mathbf{k}$) by an azimuthal low-pass filter:

$$.P(\mathbf{k}) = \exp(-k_y^2/k_c^2)\, F(\mathbf{k})$$

Realizations of the ocean wave fields and SAR image intensity fields are generated from the corresponding spectra by using random phases (according to a uniform pdf). The phases of the waves are chosen at random, but for each example shown they are the same random choice.

Simulations have been carried out for two cases: (1) a Jonswap spectrum and (2) a combination of a Jonswap spectrum and a swell spectrum (a Gaussian as function of angular frequency ω and direction θ).

In the first example the ocean wave field consists of a wind sea with a peak frequency of 0.11 Hz, a wave height of 3.5 m and a mean wave direction which is 45 deg. from the range direction. Results of the simulations are depicted in Fig. 4.The panels on the left show the wavenumber spectrum of the sea surface elevation (top panel) and the wavenumber spectrum of SAR image intensity (lower panel),where the k_x direction corresponds to the range direction. The panels on the right show the sea surface elevation map (top panel) and the corresponding SAR image intensity map (bottom panel). The azimuthal cutoff wavelength (determined from the third equation of Section 3.3) is in this case $\lambda_{min} = 229$ m. This example clearly shows that the group structure of the sea surface elevation field and the SAR image intensity field are quite different and that velocity bunching rotates the waves towards the range direction.
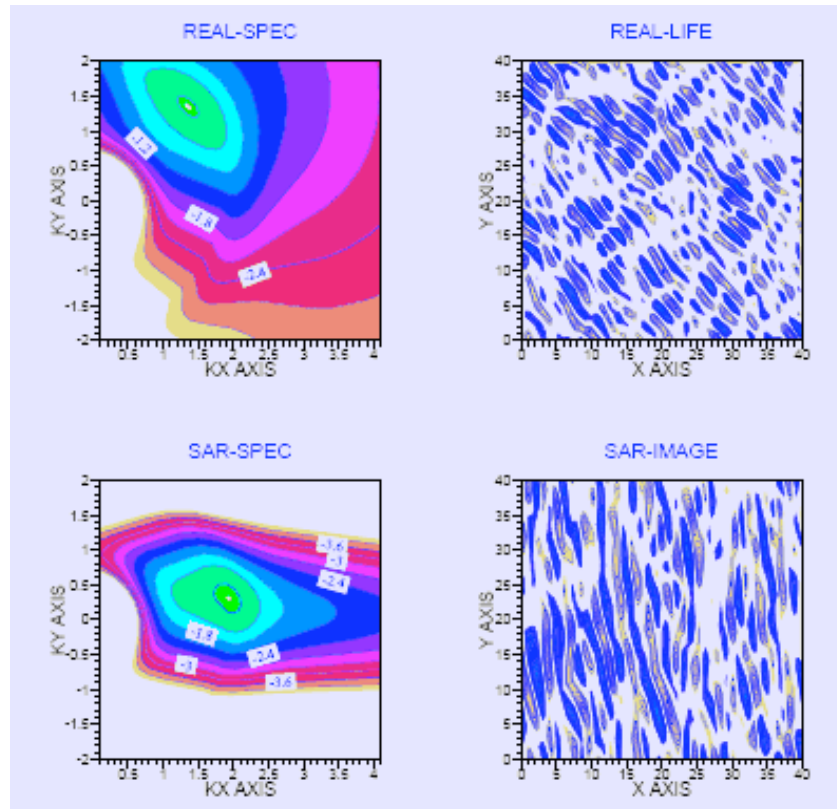
Fig.4: Comparison of a sea surface elevation map with the corresponding simulated SAR image intensity map (right panels). In the left panels the corresponding ocean wave and SAR image intensity spectra are shown. Imaged is a wind sea with mean wave direction of 45 deg. from the range direction. The azimuthal cutoff wavelength is 229 m. The x-direction is the range direction.

In the second example the ocean wave field consists of crossing seas, a case which is thought to have some relevance for freak wave generation. Here, the wind sea is the same as in the previous example, but we have added a narrow-band swell travelling in range direction. The significant wave height is now 4.94 m, while the peak frequency of the swell is 0.08 Hz. While in reality (top right panel) we see a fairly chaotic sea state mainly propagating in the wind sea direction, the SAR image shows, on the other hand, a coherent pattern propagating in the range direction, thus giving a completely false picture of reality.
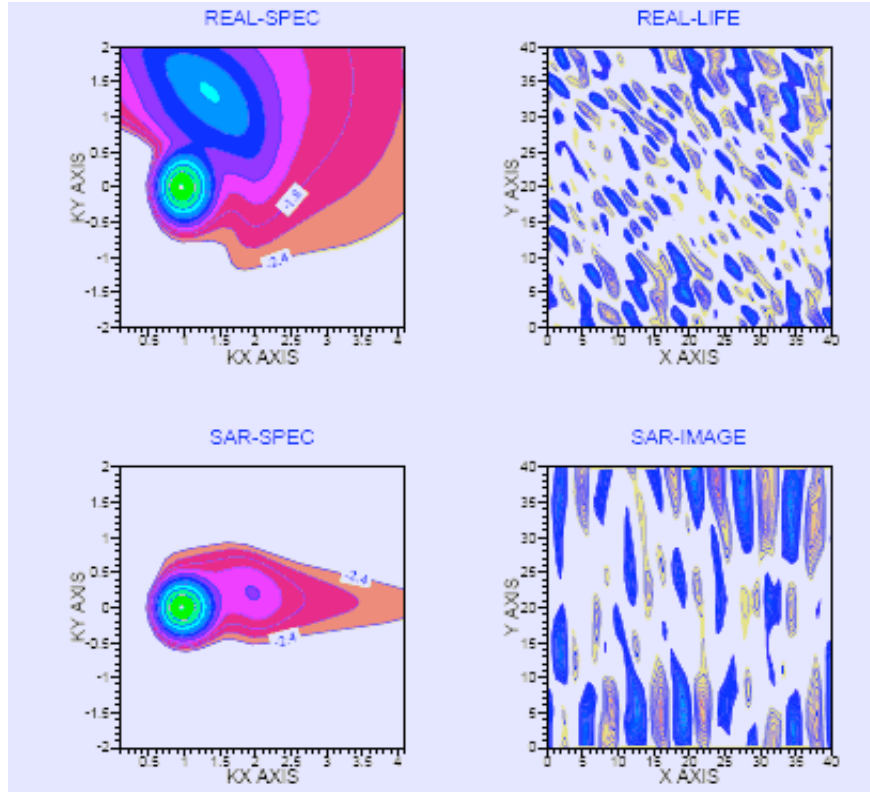
Fig.5: Comparison of a sea surface elevation map with the corresponding SAR image intensity map (right panels). In the left panels the corresponding ocean wave and SAR image intensity spectra are shown. Imaged is a wind sea with mean wave direction of 45 deg. from the range direction and a swell travelling in range direction. The azimuthal cutoff wavelength is 278 m. The x-direction is the range direction.

.

5 PEAKEDNESS OF OEAN WAVE SPECTRA

When aiming at locating extreme wave events, it desirable to have information on the width of the ocean wave spectra. Ocean wave spectra with narrow widths tend to favour the generation of extreme waves. For this purpose, ECMWF uses Goda's peakedness parameter Q_p which is defined by

$$Q_p = \frac{2}{m_0^2} \int d\omega \ \omega E^2(\omega)$$

where $E(\omega)$ is the frequency spectrum of the ocean wave field. Narrow spectra correspond to high values of Q_p.

First, Fig. 6 shows that the WAM model gives, compared to buoy data, an accurate, unbiased estimate of Q_p. Therefore, it seems that modelled ocean wave spectra could play a useful role in assessing how coherent the local sea state is, and thus provide information on the probability of the occurrence of freak waves. On the other hand, the ENVISAT level 2 ASAR wave mode products turn out to be problematic in giving good estimates of the peakedness of the ocean wave spectra. This is seen in Fig.7 where peakedness from the Envisat level 2 ASAR wave mode product is compared with the corresponding counterpart from the WAM model. Evidently, spectra from Envisat level 2 products are too narrow. Note that the same applies also to the directional width $\Delta\theta$. This confirms our expectation from the previous section that, because of the azimuthal cutoff, SAR indeed gives too narrow ocean wave spectra and therefore observes a too coherent sea state. Thus ocean wave spectra derived from the Envisat level 2 ASAR wave mode products are prone to yield a too high probability of the occurrence of freak waves.
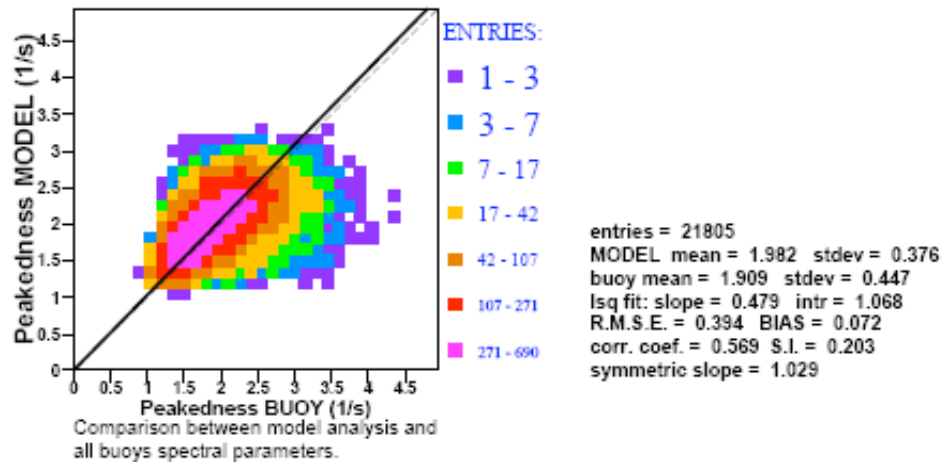
Fig.6: Comparison of modelled peakedness against buoy observations over the period October 2002 until April 2003
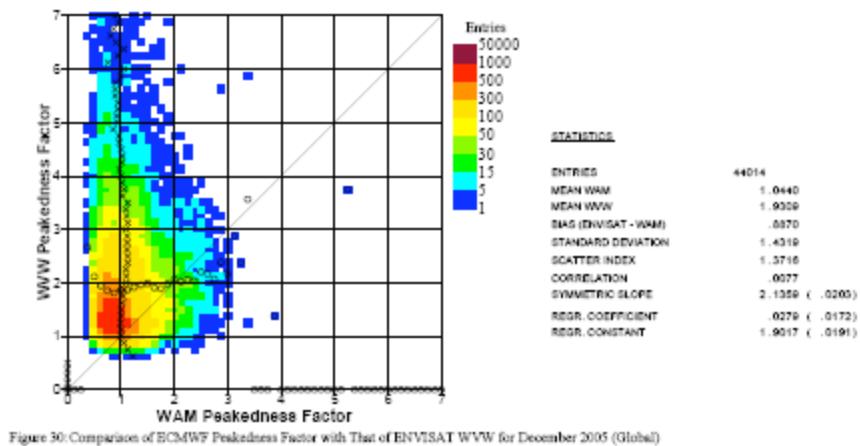
Fig. 7: Comparison of peakedness from the Envisat level 2 ASAR wave mode products with modelled peakedness for December 2005.

6 SUMMARY AND CONCLUSIONS

Recent observations of freak waves and theoretical developments on nonlinear focussing have increased our understanding of the generation of freak waves. A nonlinear, coherent sea state is most likely to generate these extreme events. This notion is supported by evidence from laboratory studies, however, validation of all this on the ocean is still required.

Observations of individual freak wave events from satellites would be most useful for the monitoring of these rare events. If these observations would exist, one would obtain important information on the frequency of occurrence of freak waves and its most likely location. In addition, it would be possible to validate existing scenarios of freak wave generation, which would be of tremendous benefit for the purpose of freak wave prediction.

Global monitoring of freak waves using the ERS SAR and ENVISAT ASAR images, in particular wave mode data, is most likely not possible, as these images give a highly distorted view of the occurence of extreme events over the global oceans. A necessary condition for freak waves to occur is that the waves are steep. This condition

most likely occurs under conditions of wind-wave generation. As soon as the wind-waves leave the storm area, wave dissipation will reduce wave steepness considerable and the eventual result is a gentle sea state called swell. Nonlinear focussing is unlikely to happen for swell. Nevertheless, SAR images only give a true picture of the sea surface under low wind conditions when swell is the dominant feature of the sea state and when it propagates close to range direction. In other cases, velocity bunching will give rise to serious distortions of the wave field.

From a freak wave forecasting perspective, all that is needed are global observations of kurtosis and skewness of the pdf of the sea surface elevation. In theory, a radar altimeter could provide this information [25], while, as indicated in this paper, also the shape of the SAR azimuthal low-pass filter might give information on non-normal aspects of the sea surface elevation pdf.

In this paper we have pointed out that the detection of several freak waves with wave heights above 25 m on ERS SAR wave mode data [4], [5], as claimed by Lehner (DLR) and Rosenthal (GKSS), has no scientific basis. Thus, unfortunately, the methods developed in their groups using ERS and Envisat wave mode data are inadequate for giving the probability of occurrence of freak waves on a global scale. The methods described in their papers [14]-[16] only apply to ocean waves that travel close to the range direction and are therefore inadequate for investigating ocean wave fields using ERS and Envisat wave mode data on a global scale since, on the World's ocean, waves are encountered that travel in all directions. ERS SAR and Envisat ASAR images most often show range travelling waves. But this is due to an artefact of the SAR imaging mechanism. Due to the nonlinearity of the SAR imaging mechanism caused by velocity bunching, ocean waves that in reality travel in off-range directions are rotated in the SAR image in the range direction. In addition, it is expected that even for range travelling waves their methods cannot be applied for detecting freak waves, because of the assumption that the modulation of the normalized radar cross section (NRCS) is linearly related to the sea surface elevation, which is most likely not be valid when SAR images extreme waves.

REFERENCES

[1] Janssen, P.A.E.M.,"Nonlinear four-wave interactions and freak waves", *J. Phys. Oceanogr.*, 33, 863-884, 2003.

[2] Alpers, W.R., and C.L. Rufenach, "The effect of orbital motions on synthetic aperture radar imagery of ocean waves", *IEEE Trans. Antennas Propagat.*, **AP-27**, 685-690, 1979.

[3] Alpers, W., D.B. Ross, and C.L. Rufenach, "On the detectability of ocean surface waves by real and synthetic aperture radar", *J. Geophys. Res., 86,* 1-6498, 1981.

[4] see the BBC film " Freak waves" from the "Horizon" programme of September 12 2002.

[5] http://www.esa.int/esaEO/SEMOKQL26WD_index_0.html ("Ship-sinking monster waves revealed by ESA satellites")..

[6] Tanaka, M, "The role of modulational instability in the formation of wave groups", in M.L. Banner and R.H.J. Grimshaw(Eds.), *Breaking waves,* 237-242, Springer Verlag, 1992.

[7] Yasuda, T., N. Mori, and K. Ito, "Freak waves in a unidirectional wave train and their kinematics",.in *Proc. 23rd Conf. on Coastal Eng.*, Venice, ASCE, vol. 1, 751-764, 1992.

[8] Yasuda, T.and N. Mori, "High order nonlinear effects on deep-water random wave trains", in *International Symposium: Waves-Physical and Numerical Modelling,* Vancouver, vol. 2, 823-832, 1994.

[9] Trulsen K., and K. Dysthe, "Freak waves: A three-dimensional wave simulation", in *Proceedings of the 21st Symposium on Naval Hydrodynamic,* National Academy Press, 550-558, 1997.

[10] Onorato M., A.R. Osborne, M. Serio, and S. Bertone, "Freak waves in random oceanic sea states", *Phys. Rev. Lett.,* 86, 5831-5834, 2001.

[11] Janssen, P.A.E.M, "Nonlinear four-wave interactions and freak waves", *J. Phys. Oceanogr.*, 33, 863-884, 2003.

[12] Mori N. and P.A.E.M. Janssen, "On kurtosis and occurrence probability of freak waves", J. *Phys. Oceanogr.*, accepted for publication, 2006.

[13] Onorato M., A.R. Osborne, M. Serio, and L. Cavaleri , "Modulational instability and non-Gaussian statistics in experimental random water-wave trains", Phys. Fluids, 17, 078101, 2005.

[14] Nieto Borge, J.C., S. Lehner, A. Niedermeier and J. Schulz-Stellenfleth " Detection of ocean wave groupiness from spaceborne synthetic aperture radar", *J. Geophys. Res.*, 109, C07005,doi:10.1029/2004JC002298, 2004.

[15] Niedermeier, A, J. C Nieto Borge, S. Lehner, and J. Schulz-Stellenfleth, "A wavelet-based algorithm to estimate ocean wave group parameters from radar images", *IEEE Trans. Geosci . Remote Sens*., 43, 327-336, 2005.

[16] Schulz-Stellenfleth, J., and S. Lehner, "Measurement of 2-D sea surface elevation fields using complex synthetic apertureradar data", *IEEE Trans. Geosci. Remote Sens.*,42(6)1149-1160, 2004.

[17] Hasselmann, K., R. K. Raney, W. J. Plant, W. Alpers, R. A. Shuchman, D. R. Lyzenga, C. L. Rufenach, and M. J. Tucker, "Theory of synthetic aperture radar ocean imaging: A MARSEN view," *J. Geophys. Res*, 90, 4659–4686, 1985.

[18] Hasselmann, K. and S. Hasselmann, "On the nonlinear mapping of an ocean wave spectrum into a synthetic aperture radar image spectrum," *J. Geophys. Res.*, 96, 10713–10729, 1991.

[19] Lyzenga, D.R., R. A. Shuchman, and J. D. Lyden, "SAR imaging of waves in water and ice: Evidence for velocity bunching," *J. Geophys. Res.,*90, 1031–1036, 1985.

[20] Bruening, C., W. Alpers, L.F. Zambresky, and D.G. Tilley: "Validation of a SAR ocean wave imaging theory by the Shuttle Imaging Radar-B experiment over the North Sea", *J. Geophys. Res.,*93, 15403-15425, 1988.

[21] Bruening, C., W. Alpers, and K. Hasselmann , "Monte-Carlo simulations studies of the nonlinear imaging of a two dimensional surface wave field by a synthetic aperture radar", *Int. J. Remote Sens.*, 11, 1695–1727. 1990.-

[22] Beal, R.C., D.G. Tilley, and F.M. Monaldo, "Large and small-scale spatial evolution of digitally processed ocean wave spectra from Seasat synthetic aperture radar", .*J. Geophys. Res.,* 88, 1761-1778, 1983.

[23] Kerbaol, V., B. Chapron, and P.W. Vachon,. "Analysis of ERS-1/2 synthetic aperture radar wave mode imagettes", J. *Geophys. Res*., 103, 7833-7846, 1998.

[24] Lyzenga, D.R., "Numerical simulation of synthetic aperture radar image spectra for ocean waves*", IEEE Trans. Geosci. and Remote Sens*., 24, 863-872, 1986.

[25] Lipa, B., and D.E. Barrick, 1981. "Ocean surface height-slope probability density function from SEASAT altimeter echo", *J. Geophys. Res*., 86, 10921-10930, 1981.